

# Triangular Profile Imprint Molds in Nanograting Fabrication

Zhaoning Yu\* and Stephen Y. Chou

*Nanostructure Laboratory, Department of Electrical Engineering,  
Princeton University, Princeton, New Jersey 08544*

*Received October 27, 2003; Revised Manuscript Received December 11, 2003*

## ABSTRACT

We have developed a technique based on nanoimprint lithography for the fabrication of nanogratings with controllable line widths and smooth edges. A wet chemical etching process is employed during mold preparation to achieve smooth line edges and a triangle-shaped grating profile. Oblique angle coating (shadow evaporation) of the imprinted resist pattern determines the grating line width. Grating duty cycles can be easily tuned from 30% to 70% of the grating period by simply changing the angle of incidence for shadow evaporation. This technique also enables us to fabricate gratings with highly smooth edges that are not easily achievable by other fabrication methods.

Nanoscale gratings have many important applications in optics, communications, biotechnology, and micro/nanofluidic devices and systems.<sup>1–4</sup> Previous fabrication methods include electron-beam lithography (EBL)<sup>5,6</sup> and interference lithography (IL).<sup>7,8</sup> However, electron-beam lithography is not suited for large-scale production of gratings due to its low throughput as a serial processing tool. In the case of interference lithography, the process latitude for grating line-width control is very limited. There have been some reports on using different exposure doses to tailor the line-width; however, the line-width/dose dependence is not linear, the tuning range is small, and the process is difficult to control,<sup>8</sup> which is further compounded by random factors in the exposure system such as disturbances and instabilities that also affect line width.

In addition to the cost associated with large-scale production, quality of the nanogratings is another important issue. In many applications, the problem of grating line-edge roughness needs to be carefully addressed. Studies have shown that edge roughness is related to the scattering loss in optical devices, it affects the electrical performances and electron transport through nanowires, and it may affect flow resistance in fluidic devices.<sup>9–11</sup>

Previous methods targeted at reducing line-edge roughness include anisotropic wet etch, thermal oxidation of sidewalls and etch back, and the optimization of dry etching parameters.<sup>9,12,13</sup> However, the applicability of those methods is limited because wet etch can be applied only to certain crystalline semiconductor materials, and thermal oxidation involves high temperature processing, which is incompatible with the materials required in many applications. Moreover, none of these approaches are aimed at reducing the edge

roughness of the original resist pattern, which serves as a mask for the following processing and directly affects the quality of the transferred pattern.

In view of the foregoing, the objective of the technology to be discussed in this paper is to provide a cost-efficient technique based on nanoimprint lithography (NIL)<sup>14</sup> for the large-scale production of nanogratings with smooth sidewalls and to provide better line width control.

Unlike previous NIL-based patterning techniques, this technique abandons the use of mold features with vertical sidewalls. Instead, it uses grating molds with triangle-shaped profiles, created on a suitable single crystalline substrate using a wet chemical etching process. The obverse of the triangular profile relief pattern on the mold is then transferred into a resist thin film by pressing the mold into the resist and removing the mold.<sup>14</sup> In subsequent steps, metal is coated onto the tips of the resist triangles through oblique-angle deposition (shadow evaporation).<sup>15</sup> Portions of the resist uncovered by the evaporated material are removed to expose the underlying substrate using reactive ion etching (RIE). The grating pattern is then transferred in the substrate by a standard lift-off<sup>16</sup> or RIE process.

Compared with previous technologies,<sup>6–8,17</sup> the triangular profile mold imprint process provides both improved line-edge smoothness and better grating line-width control, together with several other features that are important in view of large-scale production, which will be discussed in the latter part of this paper.

Figure 1 shows a schematic of the steps for the fabrication of a triangular profile grating mold. In this experiment, the mold body is made of a (100) silicon substrate, which originally has a layer of mask material (SiO<sub>2</sub>, Si<sub>3</sub>N<sub>4</sub>, etc.). The mask layer can be grown or deposited through any

\* Corresponding author. E-mail: zhyu@ee.princeton.edu

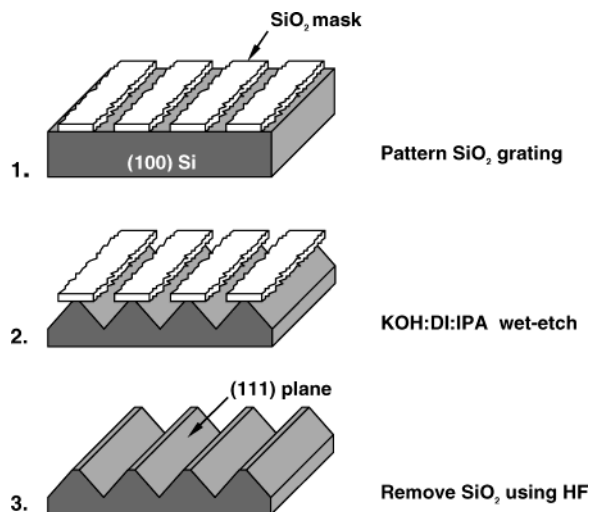


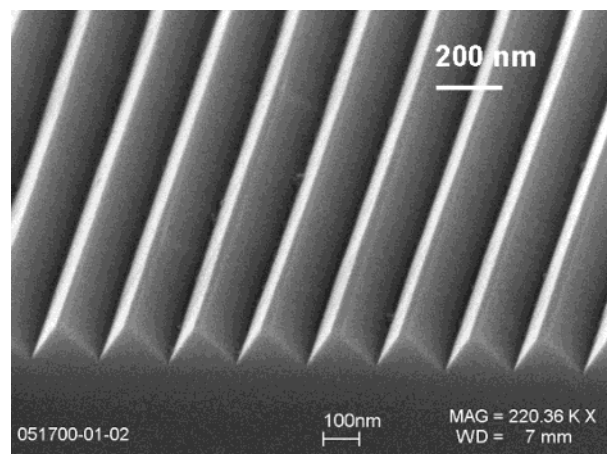
**Figure 1.** Schematic of the steps used to fabricate a triangular profile nanograting mold: (1) the mask layer carried by a (100) silicon substrate is patterned using interference lithography, the grating is aligned to be parallel to one of the (111) planes; (2) a triangular profile grating pattern is etched into the substrate using KOH-based anisotropic wet-etching; (3) the remaining SiO<sub>2</sub> is removed using diluted HF.

appropriate technique such as thermal oxidation or chemical vapor deposition (CVD). The thickness of the SiO<sub>2</sub> (or Si<sub>3</sub>N<sub>4</sub>) film typically ranges from 30 to 300 nm. The mask layer was then patterned with micro- or nanoscale grating patterns to expose part of the underlying silicon surface using a process combining interference lithography and RIE.

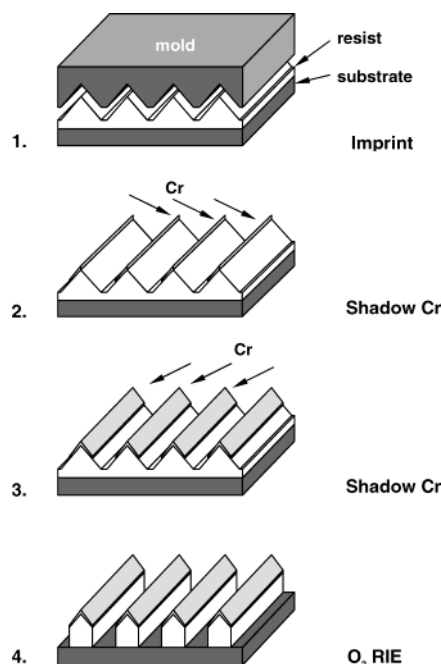
The substrate was then briefly dipped into diluted hydrofluoric acid (HF) solution to remove the oxide that may have remained in the regions between the mask lines. A mixture of 500 g potassium hydroxide (KOH), 1600 mL deionized (DI) water, and 400 mL isopropyl alcohol (IPA) heated to a temperature of 65 °C was used for the wet chemical etching step depicted in Figure 1. The optimum etching time (which ranges from 30 to 90 s for gratings with a period of 200 nm) depends on the grating period, line width of the mask, and the material of the mold body. A triangular profile mold was obtained after the remaining oxide mask was finally removed using hydrofluoric acid.

Figure 2 is a scanning electron micrograph (SEM) image of a triangular profile grating mold with a period of 200 nm created in a (100) silicon substrate using the steps described in Figure 1. Because the etching rate of silicon in the  $\langle 111 \rangle$  direction is much slower than the etching rates in the  $\langle 100 \rangle$  and  $\langle 110 \rangle$  directions,<sup>18</sup> this highly anisotropic process creates a grating structure with extremely smooth etched surfaces.<sup>19</sup>

Figure 3 shows a schematic of the steps for the patterning of resist by nanoimprint lithography with a triangular profile mold. First, a substrate with an imprint resist thin film (the resist is usually a thermal-plastic polymer that can be turned into a viscous state at elevated temperatures) is brought into contact with the mold, which is pressed into the resist after heating to allow sufficient softening of the resist. The mold is removed from the resist after cooling to leave a relief pattern in the resist, which conforms to the shape of the features on the mold.<sup>14</sup>



**Figure 2.** Scanning electron micrograph of the cross-sectional view of a triangular profile grating with a period of 200 nm etched in a (100) silicon substrate. Surfaces of the grating features are extremely smooth due to the highly anisotropic wet-chemical etching.



**Figure 3.** Schematic of the steps used to pattern the resist by nanoimprint lithography with a triangular profile mold. In this process, shadowed Cr masks the etching of the underlying resist by anisotropic O<sub>2</sub> RIE.

After the desired triangular profile is obtained in the resist, a layer of suitable mask material (Cr) is deposited onto one side of resist triangles through an oblique-angle deposition process (shadow evaporation),<sup>15</sup> which is usually complemented by another shadow evaporation step to coat the resist pattern from another side of the grating. Following the deposition of Cr, the resist in the regions unprotected by the metal mask is etched away using anisotropic O<sub>2</sub> RIE. Subsequently, the grating pattern can be replicated by lift-off<sup>16</sup> or it can be directly etched into the substrate by RIE using the shadowed Cr and the remaining resist as an etching mask.

In view of the large-scale production of nanogratings, benefits provided by a triangular profile mold include better

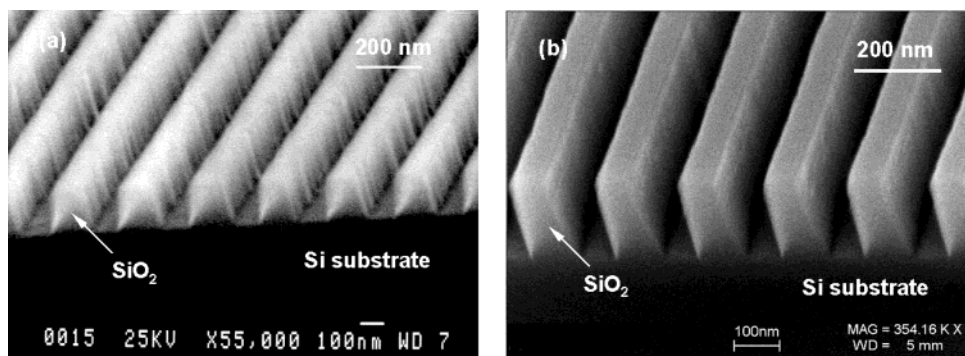


**Figure 4.** Comparison of line-edge roughness of gratings fabricated using different processes, the gratings have the same period of 200 nm, both of them are etched in a thermal oxide layer on a silicon substrate: (a) shows a grating patterned using interference lithography; the grating in (b) is patterned using the triangular mold NIL process, the edge smoothness is markedly improved.

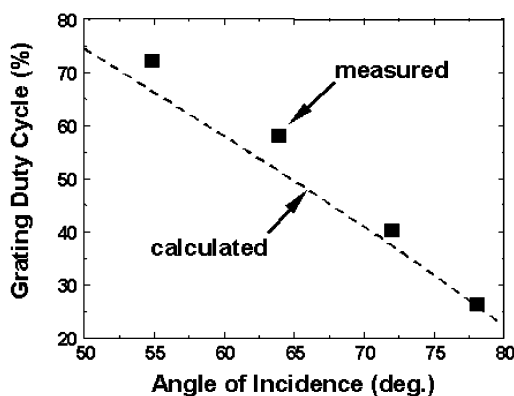


**Figure 5.** Calculated and experimentally measured grating duty cycle as a function of incident angle for shadow evaporation.

line-width control, improved line-edge smoothness, and easier mold separation. These issues will be discussed in detail in the following section.

First, since the mold is patterned by anisotropic chemical wet etch, extremely smooth (on the atomic level) sidewalls can be achieved.<sup>19</sup> The smoothness can be preserved and retained in the transferred resist pattern because of the high resolution (sub-10 nm) of nanoimprint lithography.<sup>14</sup> This process produces patterns with qualities (smoothness) unattainable by prior techniques such as interference lithography.

Figure 4 compares the line-edge roughness of gratings patterned using different processes; the gratings have the same period of 200 nm, and they were etched in a thermally grown oxide layer on a silicon substrate using the same RIE recipe. Figure 4a shows a grating patterned using interference lithography; the grating in Figure 4b, patterned using the triangular profile mold process depicted in Figure 3, shows marked improvement in line-edge smoothness.

Second, in this process, change of the grating duty cycle (which is defined as the ratio of line width/period) is achieved simply by using different angles of incidence for shadow evaporation, without the need of any modification of the mold or the imprinted resist profile. Different duty cycles can be achieved even when the same mold and imprint process are used.

Figure 5 shows the calculated and experimentally measured grating duty cycle as a function of the angle of

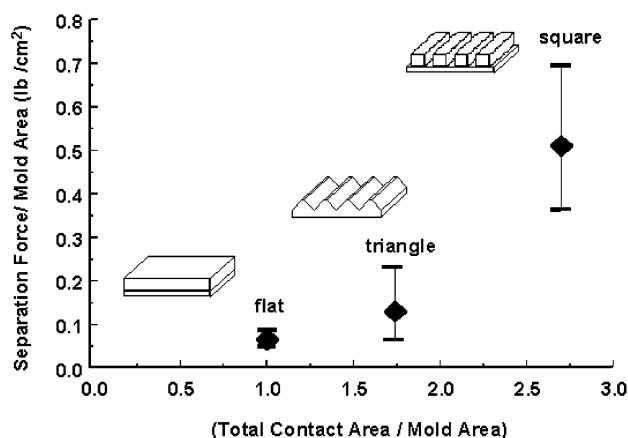


**Figure 6.** Measured peak separation force for 200 nm period grating molds with different profiles. Mold release is markedly improved in case of the triangular profile grating.

incidence for shadow evaporation. Data in Figure 5 show that the duty cycle can be easily changed over a range from 25% to 75% of the grating period, which is much wider compared to the reported range from 50% to 60% typically achieved in interference lithography.<sup>8</sup>

Third, in nanoimprint lithography, good mold release properties are important for the fabrication of nanoscale features.<sup>20</sup> By using a triangle-shaped grating profile instead of a profile with vertical sidewalls, mold release is greatly facilitated.

Figure 6 compares the measured peak separation force for molds with different profiles (flat, triangular, and square). It should be pointed out that the term “contact area” in our discussion here refers to the total area of the surface on the mold that is in contact with the imprinted resist, and the term “mold area” refers to the size of the mold. Because of the surface undulations, the contact area between mold and resist is always equal to or larger than the mold area. A reduced contact area in case of the triangular mold (compared with a square mold) contributes to a corresponding reduction in the surface energy that needs to be overcome for mold separation.

The same imprint resist (an in-house developed poly-(methyl methacrylate)-like polymer with a glass transition temperature  $T_g$  of 70 °C) was used in this experiment. The

period of the gratings is 200 nm; both the triangular and the square mold have the same feature height of  $\sim 150$  nm and they were treated together with the same mold release surfactant.

Because the actual contact area between the mold and the imprinted resist depends not only on the mold area but also on the grating feature profile, the data is plotted against the normalized contact area, which is the ratio between the mold resist contact area and the mold area.

For a flat mold, the contact area between the mold and the resist is the same as the mold area, so its normalized contact area is equal to 1.0; the normalized contact area is 1.75 and 2.75 for a triangular and a square mold, respectively. The separation force for a flat mold (with no pattern) is also plotted out for comparison. The measurement clearly indicates that the triangular profile greatly reduces the total force needed to separate the mold from the resist, compared with a mold of similar feature sizes but with a square profile.

Easier mold release helps to alleviate problems such as sticking and resist peel-off and it offers improved process latitude and flexibility in choosing a suitable imprint resist. This could prove to be a valuable characteristic for the implementation of nanoimprint lithography in the large-scale production of nanogratings.

Finally, it should be mentioned that although in our experiments we prefer to use a variety of in-house developed thermal-plastic polymers as the imprint resist, the process and principle described in this paper can also be applied using other commercially available polymers, such as poly(methyl methacrylate) (PMMA).<sup>14</sup>

In summary, we have presented in this paper an NIL-based technique suitable for the large-scale production of high-quality nanogratings with smooth sidewalls. This technique abandons the use of conventional mold features that are characterized by vertical sidewalls. Instead, a triangular profile mold is used to pattern the resist. In subsequent processing, metal coated on top of the resist pattern by shadow evaporation serves as an etching mask. Calculations and experiments show that the grating duty cycle is almost linearly dependent on the shadow evaporation incident angle.

This provides an easy method for grating line-width control. Tunable range of the grating line width is significantly increased compared to interference lithography. In addition, this technique also offers other benefits including improved mold release properties and reduced line-edge roughness, which cannot be easily achieved by using other fabrication methods.

**Acknowledgment.** The authors thank Dr. Wei Wu, Dr. Lei Chen, and Dr. Haixiong Ge for their assistance in interference lithography and the preparation of nanoimprint resists used in our experiment. This work was partially supported by DARPA and ONR.

## References

- (1) Tamada, H.; Doumuki, T.; Yamaguchi, T.; Matsumoto, S. *Optics Lett.* **1997**, *22*, 419.
- (2) Bruce, E. *IEEE Spectrum* **2002**, *39*, 35.
- (3) Austin, R. H.; Tegenfeldt, J. O.; Cao, H.; Chou, S. Y.; Cox, E. C. *IEEE Trans. Nanotechnol.* **2002**, *1*, 12.
- (4) Kim, J.; Kim, C. J. *Proc. IEEE Conf. MEMS*, 479 (Las Vegas, 2002).
- (5) Fischer, P. B.; Chou, S. Y. *Appl. Phys. Lett.* **1993**, *62*, 2989.
- (6) Lim, M. H.; Murphy, T. E.; Ferrera, J.; Damask, J. N.; Smith, H. I. *J. Vac. Sci. Technol.* **1999**, *B17*, 3208.
- (7) Ross, C. A.; Smith, H. I.; Savas, T.; Schattenburg, M. L.; Farhoud, M.; Hwang, M.; Walsh, M.; Abraham, M. C.; Ram, R. J. *J. Vac. Sci. Technol.* **1999**, *B17*, 3168.
- (8) Farhoud, M.; Ferrera, J.; Lochtefeld, A. J.; Murphy, T. E.; Schattenburg, M. L.; Carter, J.; Ross, C. A.; Smith, H. I. *J. Vac. Sci. Technol.* **1999**, *B17*, 3182.
- (9) Lee, K. K.; Lim, D. R.; Kimerling, L. C.; Shin, J.; Cerrina, F. *Optics Lett.* **2001**, *26*, 1888.
- (10) Csontos, D.; Xu, H. Q. *Appl. Phys. Lett.* **2000**, *77*, 2364.
- (11) Cao, H.; Yu, Z.; Wang, J.; Tegenfeldt, J. O.; Austin, R. H.; Chen, E.; Wu, W.; Chou, S. Y. *Appl. Phys. Lett.* **2002**, *81*, 174.
- (12) Juan, W. H.; Pang, S. W. *J. Vac. Sci. Technol.* **1996**, *B14*, 4080.
- (13) Ren, F.; Pearton, S. J.; Lothian, J. R.; Abernathy, C. R.; Hobson, W. S. *J. Vac. Sci. Technol.* **1992**, *B10*, 2407.
- (14) Chou, S. Y.; Krauss, P. R.; Renstrom, P. J. *Science* **1996**, *272*, 85.
- (15) Flanders, D. C. *J. Vac. Sci. Technol.* **1979**, *16*, 1615.
- (16) Ryan, R. W.; Kopf, R. F.; Hamm, R. A.; Malik, R. J.; Masaitis, R.; Opila, R. *J. Vac. Sci. Technol.* **1998**, *B16*, 2759.
- (17) Cavallini, M.; Biscarini, F. *Nano Lett.* **2003**, *3*, 1269.
- (18) Price, J. B. *J. Electrochem. Soc.* **1973**, *120*, C96.
- (19) Wind, R. A.; Hines, M. A. *Surf. Sci.* **2000**, *460*, 21.
- (20) Scheer, H.; Schulz, H.; Hoffmann, T.; Sotomayor Torres, C. M. *J. Vac. Sci. Technol.* **1998**, *B16*, 3917.

NL034947L